

On Recurrent Neural Networks for Sequence-based Processing in Communications

Daniel Tandler, Sebastian Dörner, Sebastian Cammerer, and Stephan ten Brink

Institute of Telecommunications, Pfaffenwaldring 47, University of Stuttgart, 70659 Stuttgart, Germany

Abstract—In this work, we analyze the capabilities and practical limitations of neural networks (NNs) for sequence-based signal processing which can be seen as an omnipresent property in almost any modern communication systems. In particular, we train multiple state-of-the-art recurrent neural network (RNN) structures to learn how to decode convolutional codes allowing a clear benchmarking with the corresponding maximum likelihood (ML) Viterbi decoder. We examine the decoding performance for various kinds of NN architectures, beginning with classical types like feedforward layers and gated recurrent unit (GRU)-layers, up to more recently introduced architectures such as temporal convolutional networks (TCNs) and differentiable neural computers (DNCs) with external memory. As a key limitation, it turns out that the training complexity increases exponentially with the length of the encoding memory ν and, thus, practically limits the achievable bit error rate (BER) performance. To overcome this limitation, we introduce a new training-method by gradually increasing the number of ones within the training sequences, i.e., we constrain the amount of possible training sequences in the beginning until first convergence. By consecutively adding more and more possible sequences to the training set, we finally achieve training success in cases that did not converge before via naive training. Further, we show that our network can learn to jointly detect and decode a quadrature phase shift keying (QPSK) modulated code with sub-optimal (anti-Gray) labeling in one-shot at a performance that would require iterations between demapper and decoder in classic detection schemes.

I. INTRODUCTION

The huge success of deep learning (DL) and NNs, mainly in the fields of computer vision and speech processing, has recently triggered further exploration of DL for communications. The potential applications span from trainable channel decoders [1], [2], [3], [4], [5], NN-based multiple-input multiple-output (MIMO) detectors [6] and detectors for molecular channels [7] up to communication systems that inherently learn to communicate [8]. Most of these applications typically rely on block-based signal processing, which is an obvious consequence if NN structures are used that were derived from computer vision tasks. Besides, those structures also benefit from the possibility of straightforward stochastic gradient descent (SGD)-based training.

In the contrary to that, signal processing for communications often benefits from sequence-based processing (e.g., a simple finite impulse response (FIR) filter for equalization) as it allows to maintain an internal state. Mainly driven by the speech processing community, a rich variety of different sequence-based RNN structures emerged, which can typically also be trained by SGD when truncated back-propagation through time (BPTT) is used. In [9], advantages for detection over molecular channels have been reported and the authors of [3], [10] show

that RNNs can improve the performance of channel decoding and also code design [11]. In this work, we aim to compare different families of RNN architectures with fundamentally different properties (e.g., NNs with external memory) rather than minor implementation differences (e.g., GRU vs. long short-term memory (LSTM)). This is also supported by [12] as the authors have shown by exhaustive search that the average performance of the GRU or LSTM cell structure does not significantly differ [12].

Besides their simple encoding structures, convolutional codes benefit from the availability of an ML decoder, namely the well-known Viterbi algorithm [13]. Thus, convolutional codes allow an easy benchmark by providing a clear (and optimal) baseline to analyze the influence of encoding memory and traceback-length, i.e., how close can a given NN approximate the optimal decoder for specifically chosen constraints.

The universal approximator theorem [14], and the fact that an explicit optimal algorithm exists, directly tells us that also an NN must exist (neglecting any complexity constraints) which comes arbitrarily close to the optimal performance. While other groups already showed the existence of such decoding NNs for short memory convolutional codes [2], [3], we want to further investigate to what extent NNs are capable of processing even more complex information sequences using the example of decoding convolutional codes up to memory ν . However, in practice the limiting factor is clearly the training complexity and, thus, the major challenge is to find a suitable training method for this task. We want to point out that the aim of this work is *not* to outperform the Viterbi decoder, but to provide insights into a suitable training methodology and efficient NN architectures for continuous signal processing in communications. Yet, a potential benefit can be seen in other metrics like the possibility of *learning to approximate* a (sub-optimal but) low-complex decoder for prohibitively large encoding memories (cf. the *NASA Big Viterbi Decoder* [15]).

In [5], it has been shown for block-codes, that NNs are limited by an exponential training complexity when training with all possible codewords is required, i.e., for k information bits 2^k different codewords needed to be shown during training. In the case of convolutional codes there is a naturally limited length that still allows (close to) optimal decoding (cf. *traceback length* in Viterbi decoding [16], [17]).

Moreover, we believe both NN structures and the training procedure, as shown for convolutional codes in this paper, are of significant practical importance in many other deep-learning-based communication applications like equalization,

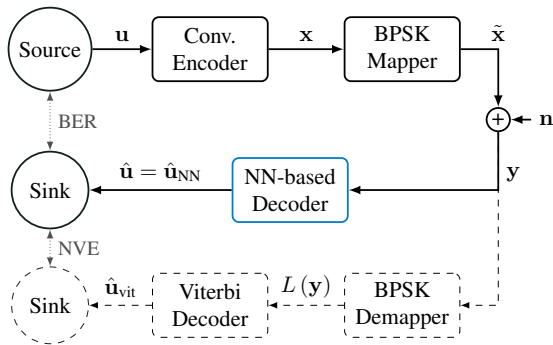


Fig. 1: System model

continuous channel state information (CSI) prediction and also with regard to the scalability of autoencoder-driven systems [8].

II. SYSTEM MODEL AND NEURAL NETWORK ARCHITECTURES

Due to many breakthroughs and rapidly increasing research in machine learning for various domains, many different network structures and concepts have emerged. When taking a closer look at the characteristics of most signals in the domain of communications we find:

- Sequences: signals are sequential, but can be often processed in a block-wise manner (cf. traceback).
- Locality: Single samples are heavily entangled in time, but, unlike sentences or audio speech (where complex context connections over long time distances occur) these dependencies – with limited memory – are short and often constant in time (tapped delay, multidimensional modulation, sampling effects).
- Complex-valued: Their dimensionality is either a single or multiple parallel complex-valued streams of samples that can be represented by concatenating real and imaginary values.

Therefore, by seeking the optimal NN structure, we focus on recurrent sequence-to-sequence models. As we chose to exemplarily decode convolutional codes, our input signals for the decoding NN are of the following properties:

- Two received samples represent one uncoded bit, as we consistently use rate $r = 1/2$ codes throughout this work.
- The original information of the uncoded bit is diffused over several received samples depending on the memory ν of the applied convolutional code. As a rule of thumb, the affected sequence is of length “traceback” [16], [17] $\ell_{\text{tb}} \approx 5 \cdot (\nu + 1)$.

Fig. 1 depicts our basic system model where a convolutional encoder maps a stream \mathbf{u} of uncoded bit $u_k \in \{0, 1\}$ to a stream \mathbf{x} of coded bit $x_k \in \{0, 1\}$, a mapper that maps those coded bits to a stream $\tilde{\mathbf{x}}$ of binary phase shift keying (BPSK) symbols $\tilde{x}_k \in \{-1, 1\}$, an additive white Gaussian noise (AWGN) channel with output $\mathbf{y} = \tilde{\mathbf{x}} + \mathbf{n}$, where $\mathbf{n} \sim \mathcal{N}(0, \sigma^2)$, and finally the NN decoder that predicts $\hat{\mathbf{u}}$, defined as $\hat{u}_k \in \{0, 1\}$, given \mathbf{y} by inherently adopting a demapping scheme. It also shows the Viterbi baseline system

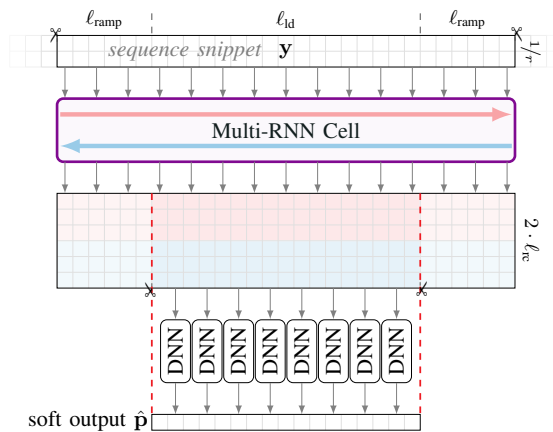


Fig. 2: Neural network based decoder architecture.

in dashed lines, where $L(\mathbf{y})$ are the log-likelihood ratio (LLR) values of \mathbf{y} and $\hat{\mathbf{u}}_{\text{vit}}$ is the estimate of the Viterbi decoder.

A. Basic Neural Network Decoder Architecture

Based on reported experiences [3], [9], [11], [10] while facing similar processing problems, and also confirmed by our own empirical experiments, we finally arrived at a baseline decoder layer architecture that makes use of bidirectional state propagation, i.e., processing the sequence from both sides.

Fig. 2 depicts our final NN-based decoder architecture which essentially consists of an RNN part in the early layers and a dense neural network (DNN) part in the later layers. As can be seen, the input to the decoder is a *sequence snippet* $\mathbf{y}^{(2\ell_{\text{ramp}} + \ell_{\text{id}}) \times 2}$ of $2\ell_{\text{ramp}} + \ell_{\text{id}}$ time steps, each containing two noisy channel observations y due to the rate $r = 1/2$ code¹. Each time step is sequentially processed in forward and backward direction by a *multi-RNN cell*, i.e., a higher level cell structure consisting of several RNN layers. While the output of the multi-RNN cell for each time step consists of ℓ_{rc} values (inspired by [2]), the cell’s outputs from both directions are concatenated for each time step. The intuition behind this procedure is to interpret the RNN output as a *latent feature* variable which then needs to be further transformed into the decision on bit \hat{u}_k . To mitigate degrading effects during state build up at the beginning and, since we are processing bidirectionally, at the end of the original input sequence, we discard the beginning ℓ_{ramp} “ramp-up” and the last ℓ_{ramp} “ramp down” time step outputs. Hence, the output tensor of the decoder’s recurrent part is of shape $\ell_{\text{id}} \times 2\ell_{\text{rc}}$.

Note that this can be straightforwardly extended to a *stateful* architecture (at least in forward direction) that promises a higher throughput by passing the forward state from sequence-to-sequence instead of discarding it. The intuition behind is to avoid the rebuild of the *internal state* of the decoder similar to the traceback in Viterbi decoding. We do not follow this approach as it heavily complicates feeding and backward direction processing while not gaining significantly in terms of

¹We assume $1/r$ is integer, which is typically the case for convolutional codes due to their encoder structure. Otherwise we suggest feeding $\lceil 1/r \rceil$ channel observations per time step while either repeating observations or zero padding observations at every second time step.

the final BER. One should also note that both designs based on bidirectional processing, stateless and stateful, exhibit a structural decoding delay of at least ℓ_{ramp} time steps, caused by the backward processing branch.

The output of the multi-RNN cell is then forwarded to a DNN layer with N_{DNN} units and exponential linear unit (ELU) activation function. This DNN layer has no connections through time and is simply meant to combine the “features” that were extracted by the preceding multi-RNN cell in forward and backward direction. Finally, the combining layer’s output tensor of shape $\ell_{\text{id}} \times N_{\text{DNN}}$ is fed into a sigmoid activated layer with only one single neuron to give an estimate $\hat{p}_k = P(\hat{u}_k = 1)$, i.e., on the soft-value of \hat{u}_k . Thereby, the final output of our NN based decoder is the vector $\hat{\mathbf{p}}^{\ell_{\text{id}} \times 1}$ which can be hard decided for BER calculations to $\hat{\mathbf{u}}$, where $\hat{u}_k = \mathbb{1}_{\{\hat{p}_k > 0.5\}}$ and $\mathbb{1}_{\{x > \delta\}}$ denotes the indicator function, i.e., returns 1 if $x > \delta$ and 0 otherwise.

B. Recurrent Neural Network Cell Structures

As illustrated by Fig. 2, the core element within our decoder architecture is the recurrent part, namely the multi-RNN cell. Thus, it is of great importance to find a good structure of these RNN layers to build up this multi-RNN wrapper cell. Such an RNN cell must be capable of generalizing to the task, while still complying to certain complexity constraints to be able to fully train the decoder within a reasonable amount of time. Out of the broad selection of NN structures available, we investigate the most promising ones for our task:

1) *Fully Connected Dense Layers (DNNs)*: To provide a fair comparison to non-recurrent networks, we also investigate *classical* feed-forward DNNs without any connections through time. Thereby, we distinguish between feeding only a single time step to the DNN to make a prediction on a single bit (as sanity check), which will not work because the DNN has no memory nor recurrent connections through time, and feeding a *snippet* of several time steps to give a prediction on several bits.

2) *Temporal Convolutional Networks (TCNs) and Trellis-nets*: Conventional convolutional neural networks (CNNs) have been mainly used in multidimensional applications, e.g., image classification. However it has recently been shown [18], that they can be successfully applied to one-dimensional sequence-to-sequence task as well, while maintaining their causality by applying a specific amount of padding to the inputs of the convolutional layers. The use of convolutional layers in TCNs² leads to parameter-sharing across layers, i.e., the number of parameters is independent of the length of the input sequence. TrellisNets [19] are an extension of TCNs with the main difference being that the weights are not only shared across single layers, but also between all layers in the network and the input to the network is injected at each layer.

3) *Memory Augmented Neural Networks (MANNs)*: The class of MANNs extends the concept of RNNs with an external memory, with which the network can interact via some sorts

²Strictly speaking, TCNs do not belong to the class of RNNs, however, we believe it is worth analyzing these sequence-to-sequence models.

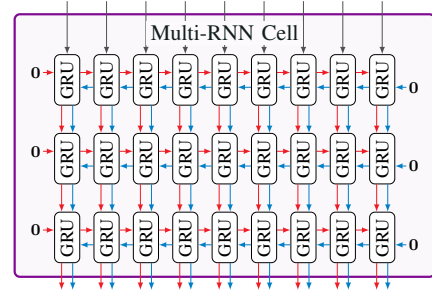


Fig. 3: Final Multi-RNN cell based on GRUs.

of interfaces. One prominent example of a MANN is the DNC [20]. DNCs use a controller, consisting of a traditional feedforward network or recurrent network, to interact with the external memory via read-and write heads. A read-head can read from the memory at each time-step while write-heads can write to the memory at each time step. All operations performed within the DNC are fully differentiable, leading DNCs to be trainable with BPTT. Thus, we use DNCs with DNN- and GRU-based controllers, denoted as DNC-(DNN) and DNC-(GRU), respectively.

4) *“Classical RNNs”: GRUs [21] and LSTMs*: As will be shown in the results, these cell structures provide sufficient complexity to solve the task while outperforming all other recurrent structures we tested in terms of low complexity and training convergence speed. The GRU-based multi-RNN cell used for all experiments throughout this work is depicted in Fig. 3. It consists of 3 GRU layers with 256 units per layer and hyperbolic tangent (tanh) activation function. One further advantage is the availability of CuDNN (an Nvidia library) implementations within the tensorflow library that are highly optimized for graphical processing unit (GPU) computations. We observe a reduction of up to factor 100 in training time compared to other RNN implementations. This renders the possibility of more training steps within the same amount of time. We also chose to use GRUs over LSTMs due to the implementational ease of only holding one internal state.

III. TRAINING METHODOLOGY

We now provide some insights in different training strategy approaches. All presented results of this section’s experiments are based on decoding the standard non-systematic memory $\nu = 6$ convolutional code $(0133, 0171)_6$.

A. Deep Learning Basics

1) *Loss Function*: As we want the NN to give an estimation of whether a bit was 0 or 1, we face a binary classification problem where the NN’s output is a vector of probabilities $\hat{\mathbf{p}} = [P(\hat{u}_1 = 1), P(\hat{u}_2 = 1), \dots, P(\hat{u}_{\ell_{\text{id}}} = 1)]$. Thus, we define the loss J as binary cross-entropy (or log-loss) function

$$J_{\log} = - \sum_{k=1}^{\ell_{\text{id}}} u_k \cdot \log \hat{p}_k + (1 - u_k) \cdot \log (1 - \hat{p}_k) \quad (1)$$

where ℓ_{id} is the length of the bit sequence that is contributing to the loss (loss depth). By introducing $\ell_{\text{id}} > 1$ we speed

up the training procedure by reducing state ramp-up overhead that would otherwise occur by simply increasing the amount of N samples within a mini-batch. This also increases the final BPTT depth of the gradient, which is at least of depth ℓ_{ramp} and at most of depth $\ell_{\text{ramp}} + \ell_{\text{ld}} - 1$ time steps.

2) *Optimizer and Learning Rate*: Both the RMSProp and Adam optimizer were tested, with RMSProp delivering slightly better results if (1) is used and Adam if the L2 loss is used, respectively. Throughout this work, we opt for a slow learning rate of $\eta = 10^{-4}$.

3) *Metrics*: The most obvious metric, besides loss, to evaluate the performance of the NN-based decoder is the BER. We calculate the BER of a mini-batch by hard decision as in

$$\text{BER} = \mathbb{E} \left[\frac{1}{\ell_{\text{ld}}} \sum_{k=1}^{\ell_{\text{ld}}} \mathbb{1}_{\{(\hat{p}_k > 0.5) \neq u_k\}} \right]. \quad (2)$$

As our decoder predicts ℓ_{ld} bits at once in a sample, one has to take care of the individual BER of each bit during architecture design. The BER of a specific bit within a mini-batch is calculated by

$$\text{BER}_k = \mathbb{E} \left[\mathbb{1}_{\{(\hat{p}_k > 0.5) \neq u_k\}} \right] \quad (3)$$

and, therefore, a significant inequality of BER between bits of different spatial positions (e.g., $\text{BER}_0 > \text{BER}_{\ell_{\text{ld}}/2}$) is a clear indicator that the hyperparameter ℓ_{ramp} was chosen to small.

Another informative metric is the normalized validation error (NVE) [5]. Since there exists an ML decoder, we can also evaluate our NN-based decoder's performance by normalizing its BER within a certain signal-to-noise-ratio (SNR) range to the optimal achievable BER obtained by the Viterbi decoder within this SNR range. This metric was introduced in a similar way in [5] and is defined as

$$\text{NVE}(\rho) = \frac{1}{S} \sum_{s=1}^S \frac{\text{BER}_{\text{NND}}(\rho, \rho_{\text{SNR},s})}{\text{BER}_{\text{Viterbi}}(\rho_{\text{SNR},s})} \quad (4)$$

where ρ is the design parameter of the NN that shall be investigated, ρ_{SNR} denotes the SNR and S is the number of SNR points. The NVE provides an easy to understand metric that depicts the influence of a certain parameter with respect to the optimal performance.

B. A Priori Ramp-Up Training

While convolutional codes up to memory $\nu = 4$ are easy to train with the presented NN-based decoder, we struggled (or never managed) to achieve convergence for codes with higher memory. In order to mitigate this problem we propose a pre-training method which can hopefully be adopted for many more sequence-based decoding problems, coined *a priori ramp-up* training. The basic idea is that, instead of starting the training with an equal distribution of zeros and ones in \mathbf{u} where $P_{\text{ap}}(u_k = 1) = 1/2$, we start training with a distribution that favors either zeros or ones, i.e. $P_{\text{ap}}(u_k = 1) < 1/2$. In the context of Information Theory, this is equal to lowering the entropy of the sequence snippet \mathbf{u} during the beginning of the training process and then gradually increasing the entropy

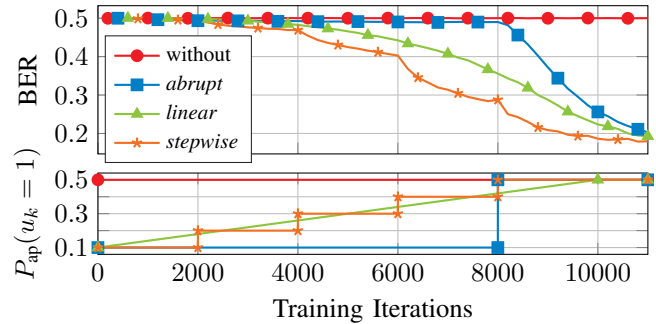


Fig. 4: BER performance at $E_b/N_0 = 1.5\text{dB}$ over the initial training iterations for different *a priori ramp-up* approaches.

of \mathbf{u} until it reaches its maximum at $P_{\text{ap}}(u_k = 1) = 1/2$. It can also be interpreted as statistically reducing the available codeword space similar to what has been done in [5] where a clear separation of codewords that have been used for training and inference was enforced. This process variably reduces complexity and, thereby, makes it easier for the NN to learn the decoding scheme in opposite to beginning training with the full codebook. The perfect amount of *a priori ramp-up* during training is still part of current research, but in the following we present three different approaches:

- *linear* – Gradually increase $P_{\text{ap}}(u_k = 1)$ for each training step.
- *stepwise* – Maintain a constant $P_{\text{ap}}(u_k = 1)$ over several training steps and then increase it after a certain criteria is reached.
- *abrupt* – Begin training at a certain constant level, e.g., $P_{\text{ap}}(u_k = 1) = 0.1$, and then, after a certain criteria is reached, we continue training at $P_{\text{ap}}(u_k = 1) = 1/2$.

Fig. 4 shows the BER performance at $E_b/N_0 = 1.5\text{dB}$ for different *a priori ramp-up* training approaches during the initial 11,000 training iterations. As can be seen from the result without the use of *a priori ramp-up* training, the NN-based decoder is not able to generalize to the problem of decoding the $(\text{o133}, \text{o171})_6$ code at all, as the BER does not decrease but constantly stays at 0.5 throughout the training. This also does not change for excessively more training iterations, because the initial *barrier-of-entry*, being the complexity of the full codebook, is prohibitively large. *A priori ramp-up* is therefore needed to initialize a learning behavior at all. This can be seen for all other approaches where *a priori ramp-up* training is used. While initially training with a low $P_{\text{ap}}(u_k = 1)$ and then *abruptly* increasing to $P_{\text{ap}}(u_k = 1) = 1/2$ is already sufficient to spark a convergence for further training at $P_{\text{ap}}(u_k = 1) = 1/2$, we can see that the *linear* and *stepwise* approaches further increase the learning speed in terms of fewer iterations needed to achieve the same BER performance. This is why we use *stepwise a priori ramp-up* training throughout this work.

C. Important Hyperparameters

1) *Layer Dimensions*: The RNN cell parameters we mention in Section II-B4 were used to decode the $(\text{o133}, \text{o171})_6$ convolutional code. For the combining DNN layer we use $N_{\text{DNN}} = 16$ units. We found out that one combining layer is

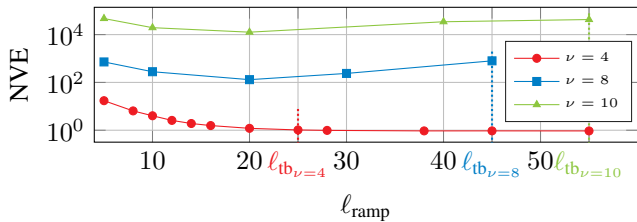


Fig. 5: Impact of *gradient depth* on the NVE performance over different ramp-up lengths l_{ramp} .

enough to do the job, more DNN layers resulted in a slower convergence during training throughout our experiments.

2) *Training SNR*: In [5] it has been empirically shown that an optimal training SNR exists for a given code and NN architecture. This has also been shown analytically later in [22]. The intuition behind is that the optimal training SNR is a trade-off between training only the code structure (i.e., the inverse encoding function in the noiseless case) and learning how to handle noisy observations. We found, empirically, that the optimal SNR during training is at the point where the convolutional code performs in a range of $\text{BER} = 10^{-1}$ to $\text{BER} = 10^{-2}$. For most of the codes we investigated, this means a training SNR range between 1dB to 1.5dB.

3) *Traceback Length*: As mentioned before, the design parameters l_{ramp} and l_{id} are highly important and must be matched to the convolutional code. While l_{id} is only used to improve training efficiency, l_{ramp} basically defines the depth of the NN’s gradient and can thereby be interpreted as the NN-based decoder’s “traceback” length [17]. To be able to achieve close to ML performance, it is important that the gradient for the predictions p_1 and p_{id} is at least l_{tb} time steps deep in both directions. We ensure this by setting the state ramp-up length to $l_{\text{ramp}} = l_{\text{tb}}$ for most of our experiments.

Fig. 5 depicts the impact of gradient depth by showing the NVE over different “traceback” lengths l_{ramp} while $l_{\text{id}} = 1$ for this experiment (to guarantee a constant gradient depth). To calculate a suitable NVE we chose $S = 8$ SNR-points equally spaced starting from $\rho_{\text{SNR},1} = 0\text{dB}$ up to $\rho_{\text{SNR},8} = 3.5\text{dB}$. As can be seen for both codes, the decoding performance heavily depends on the gradient depth and results in a bathtub curve for too complex codes with high memory ν if plotted over different l_{ramp} . It is obvious that while $l_{\text{ramp}} < l_{\text{tb}}$, the decoder can not reach ML performance, but if l_{ramp} is chosen too high, more training would be required. While $l_{\text{ramp}} \geq l_{\text{tb}}$ can easily be trained when decoding the $\nu = 4$ code, this is not possible for the $\nu = 8$ and $\nu = 10$ codes since the NN becomes too deep and complex to achieve optimal performance. Also note that we stopped training for the $\nu = 8$ and $\nu = 10$ codes after several days since there was no further improvement.

IV. RESULTS

In this Section, we will present some results which demonstrate that it is possible to process high-entropy signal with NNs, even for highly complex tasks like decoding a memory $\nu = 6$ convolutional code as used in 802.11 and many other communication standards.

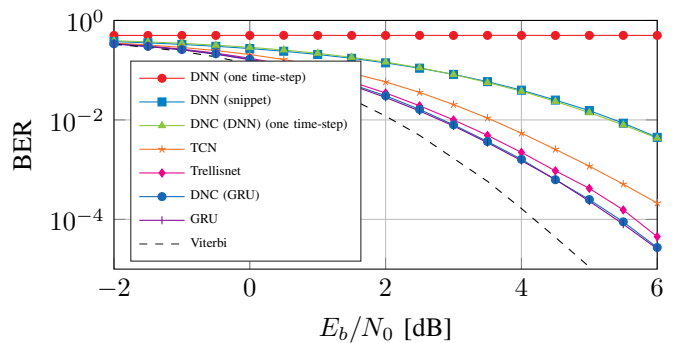


Fig. 6: BER performance of different RNN cell structures after limited training with the $(o23, o35)_4$ convolutional code.

A. Comparison Of Different RNN Cells

Fig. 6 provides a BER over SNR performance comparison of all tested RNN cell structures. The amount of training steps is fixed to 10,000 iterations and all training hyperparameters are consistent throughout all structures. We chose to present this result for the $(o23, o35)_4$ convolutional code as some structures did not converge for higher memory codes and to limit training complexity.

- 1) As can be seen the GRU-based multi-RNN cell performs best after a limited amount of training.
- 2) Also the DNC-(GRU) cell, which uses GRU-based controllers yields the same performance. However, we assume this may be mainly caused by the embedded GRU structure.
- 3) The DNC-(DNN) cell, using DNN-based controllers, performs as bad as the snippet-based DNN decoder. But this shows (and is worth mentioning), that the DNC-(DNN) must use its attached memory as we only feed one time-step y_k per decision. In contrary to the to the non-snippet based DNN (i.e., a DNN that only sees y_k per decision) this net structure is in principle able to decode and, thus, must make use of its external memory.
- 4) The Trellisnet and TCN cells also show a better convergence than the simple snippet-based forward fed DNN, which means their structure also improves signal processing for this problem.

From a rather practical perspective one of the most important problems with complex structures like the DNC-(GRU), Trellisnet and TCN cells is, that their computation time is way longer than the GRU cell’s. This means one can perform way more training iterations with a GRU-cell-based decoder than with the more complex cells in the same amount of time.

B. Achieved BERs for different convolutional codes

Fig. 7 shows the BER performance of the proposed NN based decoder for different convolutional codes. The characteristics of all investigated codes are listed in Table I. It can be seen that the NN-based decoder is able to pretty much achieve the Viterbi performance for all codes up to memory $\nu = 6$, although the performance for codes with higher memory shows

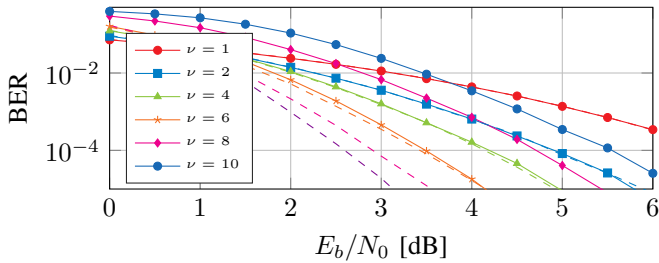


Fig. 7: BER performance of the NN-based decoder for different codes (Viterbi performance in dashed lines).

TABLE I: Characteristics of all learned convolutional codes

type	generator polynomials	code rate	constr. length ($\nu + 1$)	ℓ_{tb}
$\tilde{\text{N}}\tilde{\text{S}}\tilde{\text{C}}$	$(\text{o}1, \text{o}3)_1$	1/2	2	10
$\tilde{\text{N}}\tilde{\text{S}}\tilde{\text{C}}$	$(\text{o}5, \text{o}7)_2$	1/2	3	15
$\tilde{\text{N}}\tilde{\text{S}}\tilde{\text{C}}$	$(\text{o}23, \text{o}35)_4$	1/2	5	25
$\tilde{\text{N}}\tilde{\text{S}}\tilde{\text{C}}$	$(\text{o}133, \text{o}171)_6$	1/2	7	35
$\tilde{\text{N}}\tilde{\text{S}}\tilde{\text{C}}$	$(\text{o}561, \text{o}753)_8$	1/2	9	45
$\tilde{\text{N}}\tilde{\text{S}}\tilde{\text{C}}$	$(\text{o}2335, \text{o}3661)_{10}$	1/2	11	55

a significant gap of several dB to the optimal performance. Both results for the $\nu = 8$ and $\nu = 10$ codes are achieved by reducing the NN-based decoder’s “traceback” and, thereby, its complexity to $\ell_{\text{ramp}} = 20$. We also stopped the training process for these codes after about two days of computing time, yet Viterbi performance may possibly be reached after even more training or parallelization approaches. We still find it quite remarkable that, due to *a priori ramp-up* training, it is possible to initiate some generalization even for extremely complex convolutional codes.

V. JOINT DETECTION AND DECODING

In a bit-interleaved coded modulation (BICM) scheme with non-Gray labeling, iterations between demapper and decoder are usually required to recover the full information [23]. Thus, for anti-Gray labeling and a single demapper iteration the BER is inevitably degraded. Besides additional complexity, such iterative receiver schemes also increase the overall decoding latency significantly. In this final Section, we show that an NN-based decoder is inherently able to achieve a BER performance that could otherwise only be reached using multiple iterations over demapper and decoder. For this, we extend our system model by anti-Gray QPSK mapping.

Fig. 8 shows the NN-based decoders performance if anti-Gray labeled QPSK modulation is used. As can be seen it outperforms the non-iterative Viterbi decoder for both with and without using a bit-interleaver and even slightly outperforms the Gray labeling QPSK Viterbi performance at low SNR. As reported in [23], the Viterbi decoder using a bit-interleaver and iterative demapping and decoding with only 3 iterations then again easily performs better than the NN-based decoder. However, we want to emphasize that the NN-based decoder provides *one-shot* estimates outperforming the optimal non-iterative scheme. As in [5], we coin the term *one-shot* decoding

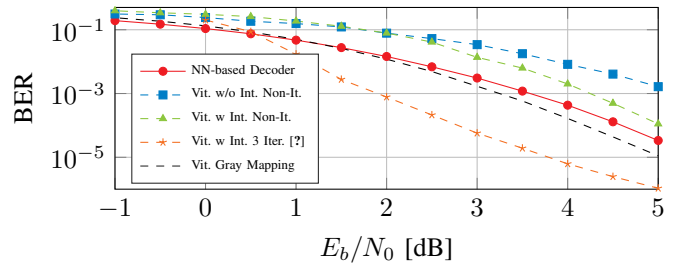


Fig. 8: BER performance of the NN-based decoder for anti-Gray mapped QPSK modulation.

as this scheme does not need any further iterations and, thus, can possibly operate at much lower overall decoding latency.

REFERENCES

- [1] E. Nachmani, Y. Be’ery, and D. Burshtein, “Learning to decode linear codes using deep learning,” in *Allerton*. IEEE, 2016, pp. 341–346.
- [2] Y. Jiang, H. Kim, H. Asnani, S. Kannan, S. Oh, and P. Viswanath, “Deepturbo: Deep turbo decoder,” *arXiv:1903.02295*, 2019.
- [3] H. Kim, Y. Jiang, R. Rana, S. Kannan, S. Oh, and P. Viswanath, “Communication algorithms via deep learning,” *arXiv:1805.09317*, 2018.
- [4] Y. Jiang, H. Kim, H. Asnani, and S. Kannan, “Mind: Model independent neural decoder,” *arXiv:1903.02268*, 2019.
- [5] T. Gruber, S. Cammerer, J. Hoydis, and S. ten Brink, “On deep learning-based channel decoding,” in *CISS*. IEEE, 2017, pp. 1–6.
- [6] N. Samuel, T. Diskin, and A. Wiesel, “Deep MIMO detection,” in *SPAWC*. IEEE, 2017, pp. 1–5.
- [7] N. Farsad and A. Goldsmith, “Detection algorithms for communication systems using deep learning,” *arXiv:1705.08044*, 2017.
- [8] T. O’Shea and J. Hoydis, “An introduction to deep learning for the physical layer,” *IEEE Transactions on Cognitive Communications and Networking*, vol. 3, no. 4, pp. 563–575, Dec 2017.
- [9] N. Farsad and A. Goldsmith, “Neural network detection of data sequences in communication systems,” *IEEE Transactions on Signal Processing*, vol. 66, no. 21, pp. 5663–5678, 2018.
- [10] W. Lyu, Z. Zhang, C. Jiao, K. Qin, and H. Zhang, “Performance evaluation of channel decoding with deep neural networks,” in *ICC*. IEEE, 2018, pp. 1–6.
- [11] Y. Jiang, H. Kim, H. Asnani, S. Kannan, S. Oh, and P. Viswanath, “Learn codes: Inventing low-latency codes via recurrent neural networks,” *arXiv:1811.12707*, 2018.
- [12] K. Greff, R. K. Srivastava, J. Koutník, B. R. Steunebrink, and J. Schmidhuber, “LSTM: A search space odyssey,” *IEEE transactions on neural networks and learning systems*, vol. 28, no. 10, pp. 2222–2232, 2017.
- [13] A. Viterbi, “Error bounds for convolutional codes and an asymptotically optimum decoding algorithm,” *IEEE Trans. Inform. Theory*, vol. 13, no. 2, pp. 260–269, 1967.
- [14] K. Hornik, M. Stinchcombe, and H. White, “Multilayer feedforward networks are universal approximators,” *Neural networks*, vol. 2, no. 5, pp. 359–366, 1989.
- [15] I. Onyszchuk, “coding gains and error rates from the big viterbi decoder,” *The Telecommun. and Data Acquisition Progr. Report 42-106*, 1991.
- [16] G. D. Forney Jr, “Convolutional codes II. Maximum-likelihood decoding,” *Information and control*, vol. 28, no. 3, pp. 222–266, 1974.
- [17] F. Hemmati and D. J. Costello, “Truncation error probability in viterbi decoding,” *IEEE Trans. Commun.*, vol. 25, no. 5, pp. 530–532, 1977.
- [18] S. Bai, J. Z. Kolter, and V. Koltun, “An empirical evaluation of generic convolutional and recurrent networks for sequence modeling,” *arXiv:1803.01271*, 2018.
- [19] —, “Trellis networks for sequence modeling,” *arXiv:1810.06682*, 2018.
- [20] Graves *et al.*, “Hybrid computing using a neural network with dynamic external memory,” *Nature*, vol. 538, no. 7626, p. 471, 2016.
- [21] K. Cho, B. Van Merriënboer, C. Gulcehre, D. Bahdanau, F. Bougares, H. Schwenk, and Y. Bengio, “Learning phrase representations using RNN encoder-decoder for statistical machine translation,” *arXiv:1406.1078*, 2014.
- [22] M. Benammar and P. Piantanida, “Optimal training channel statistics for neural-based decoders,” in *Asilomar*, Oct 2018, pp. 2157–2161.
- [23] S. ten Brink, J. Speidel, and R. H. Jan, “Iterative demapping for QPSK modulation,” *IEE Electron. Lett.*, vol. 34, no. 15, pp. 1459–1460, 1998.